CONTENTS

Structural Organogermanium Chemistry

K. C. MOLLOY AND J. J. ZUCKERMAN

Preparations and Reactions of Inorganic Main-Group Oxide Fluorides

JOHN H. HOLLOWAY AND DAVID LAYCOCK

The Chemistry of Nitrogen Fixation and Models for the Reactions of Nitrogenase

RICHARD A. HENDERSON, G. JEFFERY LEIGH, AND CHRISTOPHER J. PICKETT

Trifluoromethyl Derivatives of the Transition Metal Elements

JOHN A. MORRISON

ADVANCES IN INORGANIC CHEMISTRY AND RADIOCHEMISTRY, VOL. 27

ALKALI AND ALKALINE EARTH METAL CRYPTATES

DAVID PARKER

Department of Chemistry, University of Durham, Durham, England

I. Introduction

Until the late 1960s, whereas there had been considerable interest in the transition metal complexes of natural and synthetic macrocyclic ligands (*1–4*), relatively few reports described complexes of alkaline earth and more particularly alkali metal cations. Research in this area was stimulated by the recognition of the importance of the biological role of Na^+, K^+, Ca^{2+}, and Mg^{2+} and also the discovery and characterization of the natural antibiotic ionophores (*5, 6*). These macrocyclic antibiotics, such as valinomycin and nonactin, were shown to complex alkali metal cations with remarkable selectivity (*7–9*).

Soon after Pedersen's fortuitous discovery of the macrocyclic polyethers (crown ethers), for example **1** (*10*), Simmons and Park re-

ISBN 0-12-023627-3

ported the synthesis of a series of macrobicyclic diamines, **2** (*11, 12*). Meanwhile Lehn, prompted by the results on ionophore antibiotics, had been considering the synthesis of synthetic cyclopeptides capable of binding cations. Following Pedersen's preliminary communication

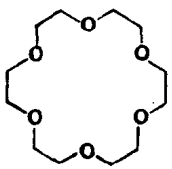

1

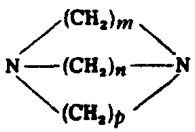

2

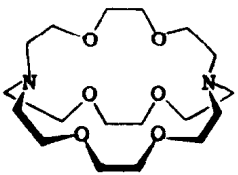

3

on the macrocyclic polyethers, the idea of synthesizing ligands with a three-dimensional cavity crystallized, leading to the development of the macrobicyclic polyethers in 1968 (*13–15*). The macrobicyclic ligand **3**, has probably been the most extensively studied of a growing number of such macrocycles.

II. Topology and Nomenclature

A. Nomenclature

Synthetic macropolycyclic ligands form inclusion complexes in which the substrate (usually a cation) is contained inside the molecular cavity (or crypt). For this reason Lehn suggested that such ligands be termed cryptands and their inclusion complexes be called cryptates[1] (*16, 17*). In order to avoid rather clumsy IUPAC nomenclature, a succinct description of the ligand is given in which the number of heteroatoms in the chains between the bridgehead atoms is given in brackets: thus, 1,13-diaza-4,7,10,13,16,19,22,27,30-octaoxabicyclo[8.11.11]-

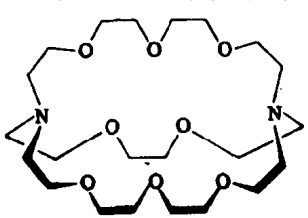

4

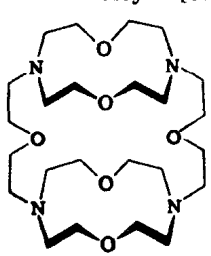

5

[1] Vogtle has suggested that synthetic ionophores be classified as follows (*21*): coronands are macromonocyclic compounds with any heteroatoms; cryptands are bi- and polymacrocyclic ligands with any heteroatoms and podands are acyclic coronand and cryptand analogs. The term crown ether is reserved for coronands with only oxygens as heteroatoms. Such a classification will be used hereafter.

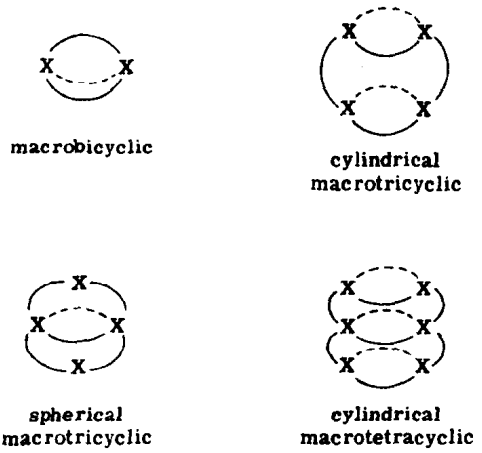

FIG. 1. Topology of cryptands.

dotriacontane becomes [3.2.2](4)(*13–15*). Macrobicyclic cryptands are often written as [2] cryptands, so that [3] cryptands are the macrotricyclic ligands such as **5** (*18–20*).

B. TOPOLOGICAL REQUIREMENTS

The topologies of various cryptands are shown in Fig. 1. Considering the macrobicyclic ligands, each bridgehead may be turned either inward or outward with respect to the molecular cavity (*11, 12, 22*). This leads to three topological isomers: exo–exo, exo–endo, and endo–endo. Crystal structures of one representative of each have been described. [2.2.2] adopts the endo–endo conformation with both nitrogen lone pairs directed into the cavity, while its bis-borane derivative is exo–exo (*23*) and the mono-borane derivative of [1.1.1] has the exo–endo form (*24*) (Fig. 2), with the $—BH_3$ group outside the cavity.

The topological requirements of cryptands which favor complexation of alkali and alkaline earth cations may be defined as follows:

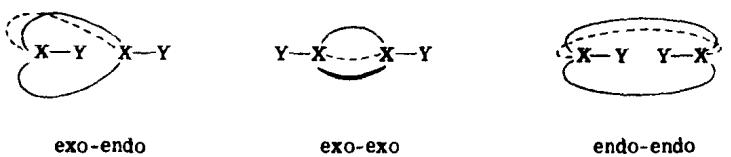

FIG. 2. Topological isomerism of cryptands. (a) X = N, Y = lone pair; (b) X = C, Y = Hor R.

1. The cryptand should define a spherical cavity with heteroatom lone pairs focusing toward the center of the cavity.
2. Ligand torsional strain should be minimized by adopting favorable antiperiplanar (180°) —C–O— and synclinal (60°) —C–C— torsion angles in the oxyethylene chains.
3. The bridgehead centers should not be so rigid as to inhibit complex formation.

Thus, it is the polyazamacrocyclic ligands developed by Lehn which have proved to be the most successful and versatile cryptands, rather than those carbon-bridgehead cryptands sought initially by Stoddart (*25–27*) which define a spheroidal cavity (e.g., **6**). On the other hand, the bridged macrocyclic polyethers developed by Parsons (*28*), such as **7**, show high complexing ability with alkali metal cations (*28–30*)

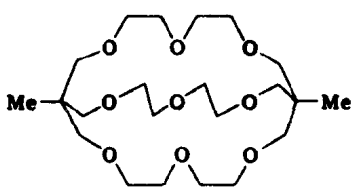

6

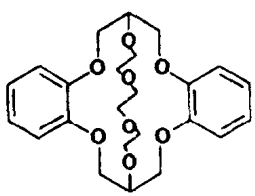

7

without exhibiting the pH sensitivity characteristic of the diazamacrobicycles.

III. Macrobicyclic Cryptates

A. Synthetic Approaches

The classical approach to [2] cryptands with bridgehead nitrogen atoms involves the high dilution reaction of a secondary bis-amine coronand with the required bis-acid chloride (*13, 14*), followed by reduction of the resultant bis-amide with diborane. Such an approach has been used to synthesize [2.2.2], for example, and also the related pyridinophane cryptand (*31, 32*) (Fig. 3). The high dilution technique requires gradual mixing (over a period of about 8 h) of reagents in order to avoid polymerization reactions, although Dye has shown that the reaction may be effected in under a minute if the reagents are efficiently mixed in a suitable flow cell (*37*). The simple approach to diazamacrocyclic ligands is in stark contrast to the rather lengthy and/or low-yielding procedures required to synthesize the cryptands with

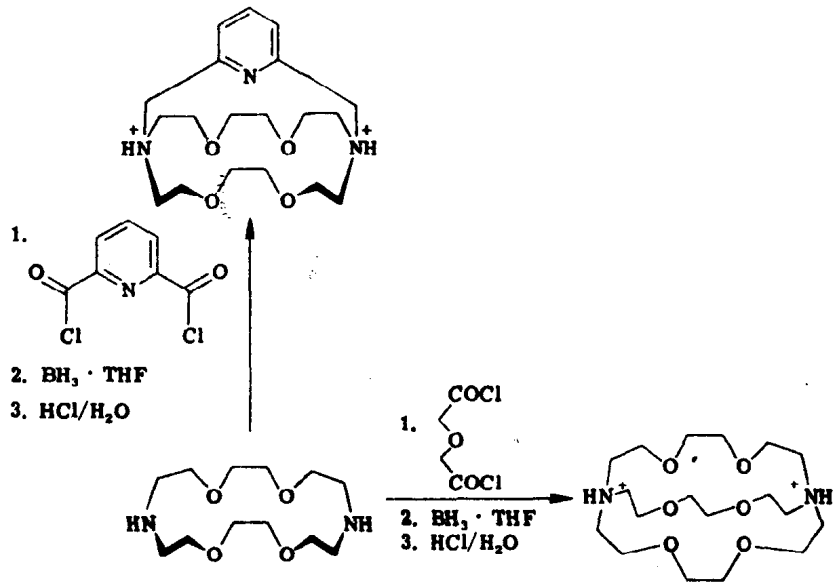

FIG. 3. Synthesis of cryptands via high dilution reaction.

carbon atoms at the bridgehead, such as **6** (*25, 30*). As a consequence of the relatively slow formation of carbon–oxygen bonds, no advantage could be gained by working at high dilution.

The synthesis of macropolycyclic cryptands generally involves stepwise, straightforward pathways (*18, 20, 33*) based on the successive construction of systems of increasing cyclic order: macrocyclic, macrobicyclic, and so on. Newkome has recently reported a satisfactory quaternization–dealkylation procedure, facilitating the synthesis of **8** (*34*). Unlike the synthetic approaches to simple crown ethers (*10,*

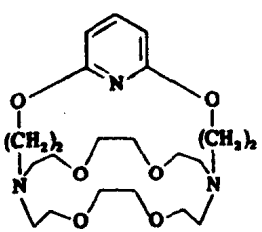

8

35), template-directed syntheses involving metal cation association have proved unsuccessful. Nevertheless, an unusual intramolecular

TABLE I

SELECTED X-RAY CRYSTALLOGRAPHIC DATA FOR METAL CRYPTATES

Cryptate[a]	Bond distances (Å) M—N	Bond distances (Å) M—O	N · · N separation[b] (Å)	Mean[c] NC–CO torsion angle (deg)	References
[2.1.1] complex					
$[Li.L]^+I^-$	2.29, 2.29	2.08–2.17	4.21	56.0	*45*
[2.2.1] complexes					
$[Na.L]^+SCN^-$	2.59, 2.70	2.45–2.52	4.94	61.6	*44*
$[K.L]^+SCN^-$	2.90, 2.92	2.76–2.87	5.14	65.5	*44*
[2.2.2] complexes					
$[Na.L]^+I^-$	2.72, 2.78	2.57–2.58	5.50	44.8	*39*
$[Na.L]^+Na^-$	2.72[d]	2.57[d]	5.43	—	*131, 132*
$([Na.L]^+)_3Sb_7^{3-}$	2.83, 2.94	2.40–2.71	5.84[d]	—	*143*
$[K.L]^+I^-$	2.87, 2.87	2.78–2.79	5.75	54.3	*38*
$[Rb.L]^+[(NCS)(H_2O)]^-$	2.99, 3.01	2.88–2.93	6.00	66.0	*41*
$[Cs.L]^+[(NCS)(H_2O)]^-$	3.02, 3.05	2.96–2.97	6.07	71.2	*41*
$[Ca.L(H_2O)]^{2+}(Br^-)_2$	2.72, 2.72	2.49–2.55	5.44	51.5	*42*
$[Ba.L(NCS)(H_2O)]^+NCS^-$					
Molecule 1	2.94, 3.00	2.75–2.82	5.94	60.6	*43*
Molecule 2	2.99, 3.00	2.74–2.89	5.94	61.5	
[3.2.2] complex					
$[Ba.L(H_2O)_2]^{2+}(NCS^-)_2$	3.08, 3.18	2.80–3.09	6.10	59.9	*46*
$(K[4.2.2])^+Cl^-$[e]	—	2.68–2.74	—	~60	*29*

[a] L = ligand.
[b] In the free ligand, N · · N = 6.87 Å (exo–exo form).
[c] In free ligand, 71.4°.
[d] Mean values.
[e] Ligand 6 with carbon bridgeheads.

hydrogen bonding effect has facilitated the synthesis of the [1.1.1] cryptand (*36*).

B. X-RAY STRUCTURAL STUDIES

As discussed in Section II,B, the nitrogen lone pairs of the [2] cryptands may be turned either inward or outward with respect to the molecular cavity, leading to three possible conformations: exo–exo, exo–endo, and endo–endo (Fig. 2). The most favorable conformation for complex formation is the endo–endo form, in which the nitrogen lone pairs are directed inward toward the metal ion. A wealth of crystallographic data exists for [2] cryptates, primarily from Weiss's group

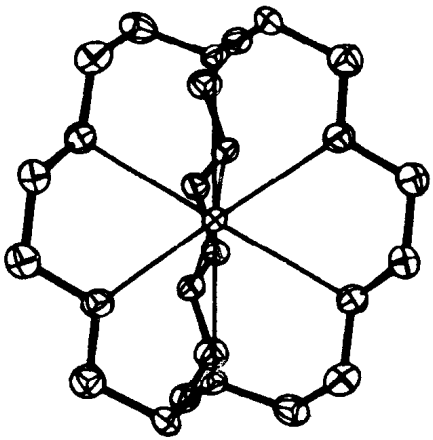

FIG. 4. Crystal structure of $(K[2.2.2])^+I^-$ (reproduced with permission).

(Table I). In all of the structures of cryptates, the ligand adopts an endo–endo conformation (*38, 39, 41–50*).

[2.2.2] Cryptates

Alkali metal complexes of the [2.2.2] cryptand afford an interesting series clearly demonstrating the conformational flexibility of the ligand to accommodate ions of differing size. The size of the cavity of the [2.2.2] cryptand (internal diameter ~2.8 Å) is close to that of the potassium and rubidium cations,[2] so that K^+ and Rb^+ cryptate formation occurs without undue ligand distortion. The structure of the potassium iodide complex is given in Fig. 4, and exhibits approximate D_3 symmetry (*38*). The potassium ion lies in the center of a trigonal antiprism with the two nitrogen atoms capping the two triangular faces and all eight heteroatoms coordinating to the cation. In this case, the anions merely occupy holes in the lattice between bulky cryptated cations. The ligand molecule in the potassium complex assumes an overall conformation of minimal strain, with favorable synclinal —C–C— and antiperiplanar —C–O— torsion angles.

[2] It has been pointed out that the size of an ion may not be specified unless the surroundings are precisely described (*40*). In this case, cryptated cations are larger than may be deduced from crystal radii because the countercharges surrounding them are lower than in the crystal lattice (an ether oxygen atom ≡ 0.15 electron charge). On the other hand, cryptand cavities are larger than ordinary van der Waals' radii indicate, as forces of attraction between cation and ligand are much stronger than ordinary van der Waals' forces.

In the corresponding complex with sodium iodide, there are some clear changes (*39*). The N · · · N distance, which is a reasonable parameter of cavity dimension, is reduced to 5.50 Å, and torsion angles about C—C and C—O bonds deviate considerably from the ideal values. The Na—N and Na—O bond distances of 2.75 and 2.57 Å are considerably larger than the sum of the Na^+ ionic radius and the van der Waals' radii of nitrogen and oxygen, respectively (2.52 and 2.42 Å). Thus the ligand undergoes a substantial deformation to accommodate the relatively small sodium ion.

The rubidium and cesium complexes of [2.2.2] are isomorphous with approximate D_3 symmetry and a crystallographic twofold rotation axis (*41*). While the rubidium cation is complexed almost without strain, the Cs^+ is accommodated only by enlarging the cavity, increasing the mean C—C torsion angle to 71° (compared with 54° for the potassium cryptate). The ligand deformations required to complex Na^+ and Cs^+ are reflected in their lower solution stability constants with respect to the K^+ and Rb^+ cryptates (see Section III,D).

In order to accommodate the small, highly charged calcium ion, the cryptand adopts an unsymmetrical conformation in which two of the chains are pushed apart to allow coordination of a water molecule and the N · · · N distance is reduced to 5.44 Å (*42*). In the corresponding barium complex, the structural unit consists of two cryptates, two water molecules, and four thiocyanate anions, two of which (**9**) are bound through nitrogen to the metal, (*43*).

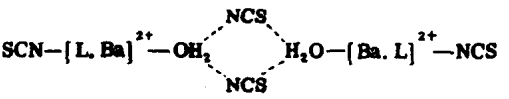

9

The [2.1.1] cryptand with six heteroatoms forms a stable LiI complex with a crystallographic twofold rotation axis as shown in Fig. 5 (*45*). The coordination about the cation describes a distorted octahedron. The [3.2.2] cryptand with one chain containing three oxygen atoms possesses a larger cavity and forms a stable barium cryptate (*46*). Unusually, the coordination number about barium is formally 11, involving the 9-ring heteroatoms and 2 water molecules. It appears that the cavity may even be too large for Ba^{2+} as the barium–nitrogen and barium–oxygen bond distances are longer than in the analogous, more stable [2.2.2] cryptate. The nonoptimal cavity size leads to a decrease in ion–dipole interaction energy which is not offset by the higher coordination number.

In the potassium cryptate with the carbon-bridgehead cryptand di-

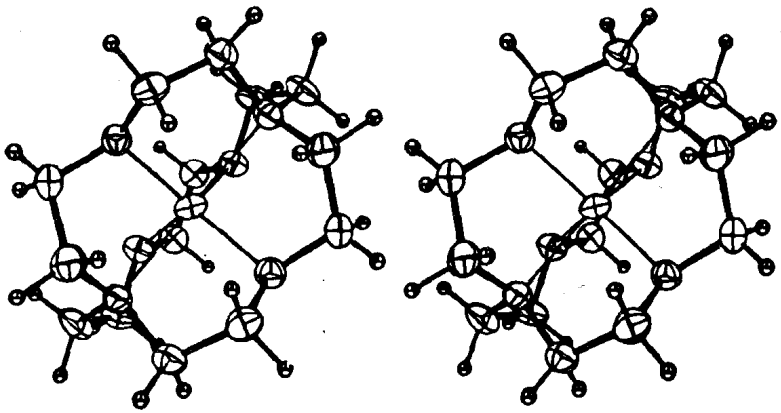

FIG. 5. X-Ray structure of $(Li[2.1.1])^+I^-$ (reproduced with permission).

benzo[4.2.2] **7**, all eight oxygen atoms are coordinated to the central cation and there are favorable C–C (~60°) and C–O (~180°) torsional angles (*29*). The structure is shown in Fig. 6. Interestingly, water molecules of crystallization and chloride anions are disordered, generating a hydrogen-bonded anionic column between the discrete cations.

Certain general features may be deduced as a result of these crystallographic investigations:

1. In all cryptates, the nitrogen lone pairs are directed into the cavity, in order to bind to the cation.

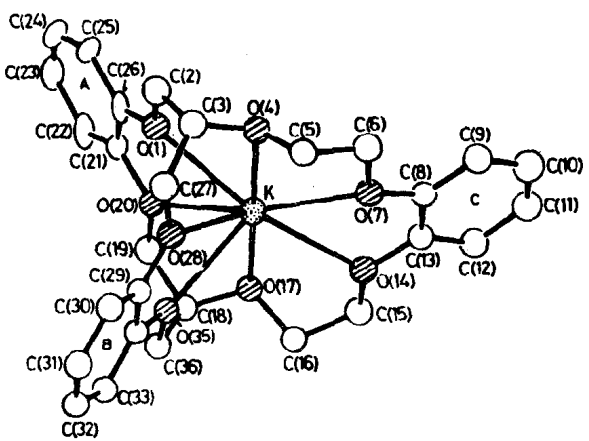

FIG. 6. Structure of the cation $(K\text{-}6)^+$; the K atom and atoms of the benzene ring A were refined with anisotropic vibration parameters (reproduced with permission).

2. With alkali metal cryptates, cations and anions are well separated (except for the KNCS complex of [2.2.1] in which the ligand is too small to effectively shield the cation). Indeed the cryptated cation may be regarded as a very large, spheroidal cation (~10 Å in diameter) of low surface charge density.

3. The alkaline earth metal cryptates have higher coordination numbers, with additional binding to solvent.

4. The cryptands are sufficiently flexible to bind very different cation sizes despite some considerable deviations of the —C↓O— and —C↓C— torsion angles from the preferred values of 180 and 60°.

C. Spectroscopic and Kinetic Studies

1. Multinuclear NMR Studies

^{1}H and ^{13}C NMR have proved to be invaluable techniques for studying the cryptands and their complexes in solution (*14, 15, 51*). Many of the cryptands are highly symmetrical and have very simple spectra which are sensitive to conformational changes on complexation. For example the ^{1}H-NMR spectrum of [2.2.2] consists of a triplet for $N—CH_2$ at 2.65δ, a singlet for $O—CH_2CH_2—O$ protons at 3.68δ, and a triplet for $—N—CH_2CH_2O$ at 3.60δ. Upon complexation, the $N—CH_2$ triplet moves upfield,[3] the shift increasing with cationic radius (*15*).

Whereas some interesting ^{15}N-FTNMR complexation studies have been carried out by Roberts (*52*), more promising results have been obtained from alkali metal NMR (*53–57*). The nuclear and spectral properties of the alkali and alkaline earth elements are shown in Table II. Despite the quadropole moment, the natural linewidths of ^{39}K, ^{23}Na, and particularly ^{133}Cs and ^{7}Li are quite narrow (under 1 Hz for the latter two). Several magnetic resonance studies using solutions of alkali salts in water and nonaqueous solvents have shown that the chemical shift of the cation is a sensitive function of its immediate chemical environment (*53, 54, 58*). Thus the nucleus of the uncomplexed ion will usually resonate at a different frequency from that of the complexed ion. In this way, addition of excess Li^+ to a solution of [2.1.1] gives two NMR signals corresponding to free and complexed ion. Exchange between free and bound lithium is slow on the NMR time scale as the lithium ion is not readily released by this cryptand. Furthermore, the limiting chemical shift of the bound Li^+ ion is almost

[3] Paramagnetic (downfield) shifts are defined as negative; diamagnetic (upfield) shifts are positive. Chemical shifts are referenced to tetramethylsilane, $\delta = 0$ ppm.

TABLE II

NUCLEAR PROPERTIES OF ALKALI AND ALKALINE EARTH CATIONS

Isotope	Spin	Relative sensitivity[a]	NMR frequency at 2.3488T (100 MHz)	Natural abundance (%)	Linewidth at half the peak height (Hz)
^{6}Li	1	8.5×10^{-3}	14.716	7.42	1
^{7}Li	$\frac{3}{2}$	0.29	38.863	92.58	1
^{23}Na	$\frac{3}{2}$	9.25×10^{-2}	26.451	100	14
^{25}Mg	$\frac{5}{2}$	2.0×10^{-3}	6.1195	10.13	7
^{39}K	$\frac{3}{2}$	5.08×10^{-4}	4.667	93.1	13
^{41}K	$\frac{3}{2}$	8.40×10^{-5}	2.561	6.88	16
^{43}Ca	$\frac{7}{2}$	6.40×10^{-3}	6.728	0.145	2
^{85}Rb	$\frac{5}{2}$	1.05×10^{-2}	9.655	72.15	150
^{87}Rb	$\frac{3}{2}$	0.17	32.721	27.85	132
^{87}Sr	$\frac{9}{2}$	2.69×10^{-3}	4.333	7.02	131
^{133}Cs	$\frac{7}{2}$	4.74×10^{-2}	13.117	100	0.6
^{135}Ba	$\frac{3}{2}$	4.90×10^{-3}	9.934	6.59	780
^{137}Ba	$\frac{3}{2}$	6.86×10^{-3}	11.113	11.32	2000

[a] On this scale $^{1}H = 1.00$, $^{13}C = 3.85 \times 10^{-6}$.

independent of solvent, indicating that the ion is effectively shielded from the solvent by the cryptand (*54*). Kintzinger and Lehn have measured ^{23}Na with 95% methanol solutions using several Na^+ cryptates (*59*). With $(Na[2.2.2])^+$, the free energy of activation for the decomplexation reaction [Eq. (1)] at 331 K is 15.4 kcal mol^{-1}, agreeing with the value obtained from ^{1}H-NMR studies (*60*). The ^{23}Na chemical shifts

$$M^+ + L \underset{k_{-1}}{\overset{k_1}{\rightleftharpoons}} (ML)^+ \qquad (1)$$

vary enormously with the cryptand. Values obtained were $+11.4\delta$ [2.2.2], $+4.25\delta$ [2.2.1], and -11.1δ [2.1.1] (relative to 0.25 *M* aqueous sodium chloride solution). In addition the calculated ^{23}Na nuclear quadropole coupling constants χ, vary linearly with the ^{23}Na chemical shifts, so that by measuring relaxation times and ^{23}Na chemical shifts a detailed study of sodium ion solvation has been made possible (*61*).

Cryptands were found to react with metal solutions in basic solvents to generate the alkali metal cryptate and an alkali anion (alkalide), for example $(Na[2.2.2])^+Na^-$ (*62*, *63*). ^{23}Na-NMR measurements of this salt in methylamine, tetrahydrofuran, and ethylamine solutions showed that the Na^- resonance is shifted strongly upfield from the Na^+ resonance (free or complexed) as shown in Fig. 7. The anion resonates at approximately the same frequency as that calculated for the free

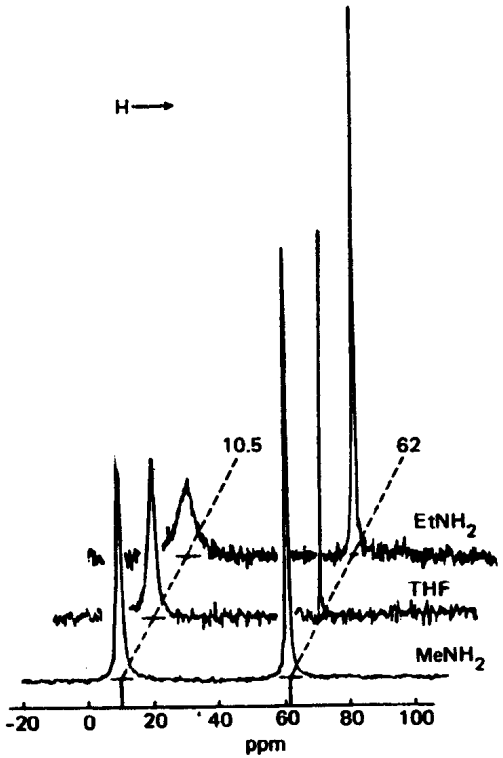

FIG. 7. ^{23}Na-NMR spectra of (Na[2.2.2])$^+$Na$^-$ solutions in three solvents (chemical shifts are referenced to Na$^+$ at infinite dilution; δ = 0 ppm) (reproduced with permission).

gaseous anion, suggesting that the anion is unsolvated. This hypothesis is confirmed by the independence of the Na$^-$ chemical shift and the nature of the solvent (*64*).

Dye and co-workers have also observed the ^{87}Rb anion in ethylamine solutions of (Rb[2.2.2])$^+$Rb$^-$. The Rb anion resonates nearly 200 ppm upfield from the aqueous Rb cation; the (Rb[2.2.2])$^+$ resonance was, however, too broad to be observed. In contrast to ^{87}Rb, natural linewidths for ^{133}Cs are very narrow, while the sensitivity is relatively high (*65, 66*) (Table II). X-Ray studies have previously shown that [2.2.2] can accommodate the large Cs$^+$, although the cavity appeared to be somewhat smaller than the size of the Cs$^+$. However, a ^{133}Cs-NMR study has revealed that in three different solvents the resonance of the complexed cation is solvent dependent so that the cation cannot be completely enclosed inside the ligand cavity (*67, 68*). As the temper-

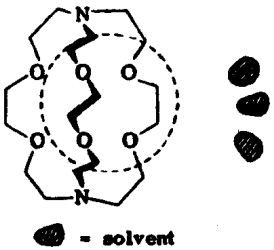

FIG. 8. An exclusive $(Cs[2.2.2])^+$ complex, (schematic).

ature is lowered, the resonance frequencies of Cs^+ in the various solvents approach the same limiting value. Such behavior is indicative of an equilibrium between two forms of the $(Cs[2.2.2])^+$ complex. This involves the "inclusive" cryptated cation which is effectively insulated from the solvent and an exclusive complex in which a partially solvated cation has relaxed out of the ligand cavity (*69*) (Fig. 8). The equilibrium [Eq. (2)] is temperature dependent, shifting to the right at

$$(Cs[2.2.2])^+_{excl} \rightleftharpoons (Cs[2.2.2])^+_{incl} \qquad (2)$$

lower temperatures. Exclusive cryptates have been observed in the crystalline state for $(K[2.2.1])^+NCS^-$ (Section III,B) in which the anion ccordinates directly to the metal.

2. *Kinetic Studies*

The kinetics and dynamics of cryptate formation (*75–80*) have been studied by various relaxation techniques (*70–75*) (for example, using temperature-jump and ultrasonic methods) and stopped-flow spectrophotometry (*82*), as well as by variable-temperature multinuclear NMR methods (*59, 61, 62*). The dynamics of cryptate formation are best interpreted in terms of a simple complexation–decomplexation exchange mechanism, and some representative data have been listed in Table III (*16*). The high stability of cryptate complexes (see Section III,D) may be directly related to their slow rates of decomplexation. Indeed the stability sequence of cryptates follows the trend in rates of decomplexation, and the enhanced stability of the dipositive cryptates may be related to their slowness of decomplexation when compared to the alkali metal complexes (*80*). The rate of decomplexation of Li^+ from [2.2.1] in pyridine was found to be 10^4 times faster than from [2.1.1], because of the looser "fit" of Li^+ in [2.2.1] and the greater flexibility of this cryptand (*81*). At low pH, cation dissociation apparently

TABLE III

KINETICS OF CRYPTATE FORMATION IN WATER

$$M^{n+} + L \underset{k_{-1}}{\overset{k_1}{\rightleftharpoons}} ML^{n+}$$

Cryptate	k_1 (M^{-1} sec^{-1})	k_{-1} (sec^{-1})	Temperature (K)	Method[a,b]	Reference
(Li[2.1.1])$^+$$ClO_4^-$	0.97×10^3	4.9×10^{-3}	298	^{7}Li NMR	*81*
(Ca[2.1.1])$^{2+}$$(Cl^-)_2$	1.6×10^2	1.6×10^2	298	SF	*80*
(Ca[2.2.1])$^{2+}$$(Cl^-)_2$	1.2×10^4	1.9×10^{-3}	298	SF	*80*
(Na[2.2.2])$^+$$Cl^-$	2×10^{5c}	27	276	^{1}H NMR	*16*
(K[2.2.2])$^+$$Cl^-$	7.4×10^{6c}	38	299	^{1}H NMR	*16*
(Rb[2.2.2])$^+$$Cl^-$	7.5×10^{5c}	38	282	^{1}H NMR	*16*
(Ca[2.2.2])$^{2+}$$(Cl^-)_2$	6.6×10^3	0.26	298	SF	*80*
(Sr[2.2.2])$^{2+}$$(Br^-)_2$	6×10^{3c}	10^{-4}	298	Pot.	*16*
(Ba[2.2.2])$^{2+}$$(Cl^-)_2$	3×10^{4c}	10^{-5}	298	Pot.	*16*

[a] SF, Stopped flow.
[b] Pot., Potentiometric data.
[c] Approximate values.

occurs via an acid-catalyzed pathway (*75*). The rates of complexation are considerably slower than diffusion-controlled rates and the transition state for this process is early, involving substantial cation solvation.

In summary, the most stable cryptates release the cation very slowly and function as cation receptors, while less stable ones undergo rapid cation exchange and may be regarded as cation carriers.

D. COMPLEX STABILITY AND CATION SELECTIVITY

The stability constants for cryptate formation [Eq. (3)] have been

$$M^{n+} + L \rightleftharpoons ML^{n+} \qquad K_c = \frac{[ML^{n+}]}{[M^{n+}][L]} \tag{3}$$

determined either by analysis of pH-metric titration curves or potentiometrically with ion-specific glass electrodes (*28, 87–89*). Some selected thermodynamic data are given in Table IV. The cryptands form the strongest known complexes of alkali metal cations, optimal stability constants being several orders of magnitude higher than with other synthetic and natural ionophores (*82*). For example, (K[2.2.2])$^+$ is about 10^4 times more stable than the natural, selective potassium ionophore, valinomycin (*83, 84*). Despite the fact that the cryptands are neutral, very stable alkaline earth cryptates are formed, and